HHS Public Access

Author manuscript

Curr Mol Med. Author manuscript; available in PMC 2015 March 23.

Published in final edited form as:

Curr Mol Med. 2014 ; 14(9): 1173–1185.

Prolylcarboxypeptidase Independently Activates Plasma Prekallikrein (Fletcher Factor)

J. Wang[1], **A. Matafonov**[2], **H. Madkhali**[1], **F. Mahdi**[3], **D. Watson**[4], **A.H. Schmaier**[5], **D. Gailani**[2], and **Z. Shariat-Madar**[*,1]

[1]Department of Pharmacology, School of Pharmacy, University of Mississippi, University, MS 38677-1848, USA

[2]Department of Pathology, Microbiology and Immunology, Vanderbilt University, Nashville, TN 37232-6307, USA

[3]Department of Pharmacognosy, School of Pharmacy, University of Mississippi, University, MS 38677-1848, USA

[4]Department of Medicinal Chemistry, School of Pharmacy, University of Mississippi, University, MS 38677-1848, USA

[5]Departments of Medicine and Pathology, Case Western Reserve University, Cleveland, ON 44106-7284, USA

Abstract

Prolylcarboxypeptidase isoform 1 (PRCP1) is capable of regulating numerous autocrines and hormones, such as angiotensin II, angiotensin III, αMSH_{1-13}, and $DesArg^9$ bradykinin. It does so by cleaving a C-terminal PRO-X bond. Recent work also indicates that the human PRCP1 activates plasma prekallikrein (PK) to kallikrein on endothelial cells through an uncharacterized mechanism. This study aims to identify PRCP1 binding interaction and cleavage site on PK. Recently, a cDNA encoding a novel splice variant of the human PRCP1 was identified. This isoform differed only in the N-terminal region of the deduced amino acid sequence. Using structural and functional studies, a combination of peptide mapping and site-directed mutagenesis approaches were employed to investigate the interaction of PRCP1 with PK. Three PRCP peptides, in decreasing order of potency, from 1) the N-terminus of the secreted protein, 2) spanning the opening of the active site pocket, and 3) in the dimerization region inhibit PRCP activation of PK on endothelial cells. Investigations also tested the hypothesis that PRCP cleavage site on PK is between its C-terminal Pro 637 (P^{637}) and Ala 638 (A^{638}). Recombinant forms of PK with C-terminal alanine mutagenesis or a stop codon is activated equally as wild type PK by PRCP. In conclusion, PRCP1 interacts with PK at multiple sites for PK activation. PRCP1 also

[*]Address correspondence to this author at the Department of Pharmacology, The University of Mississippi, University, MS 38677-1848, USA; Tel: 662-915-5150; Fax: 662-915-5148; madar@olemiss.edu.

CONFLICT OF INTEREST

The authors confirm that this article content has no conflicts of interest.

SUPPLEMENTARY MATERIAL

Supplementary material is available on the publisher's web site along with the published article.

enhances FXIIa activation of PK, suggesting that its activation site on PK is not identical to that of FXIIa.

Keywords

Diabetes; inflammation; kallikrein; hormones; obesity; renin-angiotensin system

INTRODUCTION

Prolylcarboxypeptidase isoform 1 (Accession No: NP_005031.1), is highly expressed in endothelial cells, kidney, and brain. It proteolytically inactivates vaso-active peptides bradykinin, angiotensin II, angiotensin III, and alpha melanocyte stimulating hormone (α-MSH_{1-13}) [1-3]. PRCP1 is considered to be an exopeptidase, which catalyzes the removal of an amino acid from the C terminus of a peptide with a penultimate proline.

Several serine proteases are known to liberate BK from HK: FXIIa, plasma kallikrein, activated factor XI (FXIa), and plasmin [4-8]. Plasma kallikrein has been considered to be the major BK forming enzyme from HK *in vivo*. Recent work suggests that PRCP1 activates plasma prekallikrein (Fletcher factor) [9]. PRCP1-induced PK activation on cell-bound high molecular weight kininogen (HK) causes the liberation of bradykinin (BK) from HK [9]. PK activation is reduced on PRCP1-siRNA-treated cells [10]. Since $F12^{-/-}$ mice have 50% normal BK levels, PRCP1 must be a physiological PK activator [11]. Stimulation of the angiotensin receptor 2 results in increased PRCP with increased BK formation in cultured endothelial cells [12, 13]. Since PRCP1 is recognized as an exopeptidase with substrate specificity for penultimate Pro-X bonds and PK has a C-terminal Pro-Ala bond, it has been suggested that PRCP may activate PK by cleavage of PK's C-terminus [14]. In the present study, the role of proline residues in the extreme C-terminal extension of PK in activation by PRCP is examined by an alanine scan and peptide mapping. Additionally, since a cDNA encoding a novel splice variant of the human PRCP, isoform PRCP2, was identified to have an altered N-terminus, we examined whether residues 41-140 of PRCP1 also participated in PK activation.

In this report we showed several PRCP and PK interactions sites leading to PK activation. This study also demonstrates that the N-terminus of PRCP, the C-terminus of PK and other sites participated in the binding and activation of PK by PRCP. However, cleavage of the PK C-terminal Pro-Ala bond is not essential for PRCP activation of PK. Better understanding of the structure of PRCP1 as it relates to its function has broad biological interests in cardiovascular diseases and metabolism.

MATERIAL AND METHODS

Cell culture media, PBS Dulbecco's formulation, pooled calf serum and antibiotics (penicillin and streptomycin) were purchased from Hyclone (Logan, Utah). 75 cm^3culture flasks were from Fisher Scientific (Pittsburgh, PA). Phenylmethylsulfonyl fluoride was purchased from Sigma-Aldrich Corporation (St. Louis, Mo). H-D-Pro-Phe-Arg-paranitroanilide (S2302), human HK (18 U/ml), and PK (21 U/mL) were purchased from

DiaPharma (Franklin, OH) and Enzyme Research Laboratories (South Bend, IN), respectively. H-Ala- Pro-paranitroanilide was obtained from Bachem (King of Prussia, PA). Ser-Pro-paranitroanilide was synthesized at Multiple Peptide Systems (San Diego, CA). Electrophoresis supplies and nitrocellulose membranes were obtained from Bio-Rad Laboratories (Hercules, CA). The Enhanced Chemiluminescent (ECL) detection kit was obtained from Pierce (Rockford, IL).

Peptides

As a shorthand notation, peptides were named by their first three amino acid residues and the number of amino acids present in each peptide. Peptides Ac-CKTFNQRYLVADKY-WKK-amide (CKT18) peptide corresponding to amino acids 66 to 81 and the peptide Ac-SESIHRSWDAINRLSNTC-amide (SES18) corresponding to amino acids 234 to 250 of the human PRCP1 (P42785.1) were synthesized and used as antigens to immunize goats (anti-CKT18) and rabbits (anti-SES18), respectively, at Quality Control Biochemicals-Biosource international (Hopkinton, MA). Affinity purified peroxidase conjugated mouse anti-goat and goat anti-rabbit IgG were obtained from Jackson Immunoresearch Laboratories (West Grove, Pa).Several additional peptides marching through PRCP and PK were prepared:

PRCP1 (Acc. No: NP_005031.1 or P42785.1, Full PRCP)

Five sequential 20-mers [^{41}LPAVAKNYSVLYFQQKVDH F^{60} (**LPA20**), ^{61}GFNTVKTFNQRYLVADKYWK^{80} (**GFN20**), ^{81}KNGGSILFYTGNEGDIIWFC^{100} (**KNG20**), ^{101}NNTGF MWDVAE-ELKAMLVFA^{120} (**NNT20**), and ^{121}EHRYYGE SLP FGDNSFKDSR^{140} (**EHR20**)] corresponding to amino acids 41 to 140 of the human PRCP1 were synthesized, at Quality Control Biochemicals, Bio Source International (Hopkinton, MA). In addition, two 14 to 16-mers, H-^{291}YPYASNFLQPLPAW^{304} (**YPY14**) and H-^{338}SGQVKCLNISETATSS^{353} (**SGQ16**), corresponding to amino acids 291 to 353 of the human PRCP1 were synthesized at Peptide 2.0 (Chantilly, VA).

PK (Accession No: P03952)

Five overlapping or sequential 8 to 12-mers, [H-^{384}TTKTSTRI^{391}-OH (**TTK8**), H-^{387}TSTRIVGGT^{395}-OH (**TST9**), H-^{385}TKTSTRIVGGTN^{396}-OH (**TKT12**), H-^{398}SWGEWPWQVSLQ^{409}-OH (**SWG12**), and H-^{402}WPWQVSLQVK^{411}-OH (**WPW10**)], corresponding to amino acids 384 to 411 of the human PK were synthesized. In addition, H-^{636}SPA^{638}-OH, H-^{629}DGKAQMQSPA^{638} (**DGK-10**), ^{629}DGKAQMQSAA^{638} (**DGK-10M** (M denotes modified Pro-Ala sequences) corresponding to the extreme C-terminus of PK were prepared at Multiple Peptide Systems (San Diego, CA). All peptides were purified by preparative reverse-phase high performance liquid chromatography and characterized by amino acid analysis and mass spectroscopy.

Purification of Recombinant PRCP1 (rPRCP1) from Schneider 2 Cells

rPRCP was purified according to a previously established protocol [9].

Expression and Purification of Recombinant Human Prekallikrein

cDNA for human PK was ligated into a mammalian expression vector (pJVCMV) containing a cytomegalovirus promoter. The two triplet codons in wild type PK sequence immediately preceding the 3'-stop codon code for proline and alanine. Three variants of the PK cDNA were prepared by site-directed mutagenesis so that the wild type Pro-Ala sequence was replaced by Ala-Ala (P637A), Pro-Stop (A638stop), or Ala-Stop (P637A/A638stop). HEK393 fibroblasts (ATCC-CRL1573) were transfected with 40 μg of PK/pJVCMV and 2 μg of plasmid RSVneo, containing a gene conferring resistance to neomycin. Transfection was performed by electroporation using an Electrocell Manipulator 600 (BTX, San Diego, CA). Transfected cells were grown in DMEM with 5% fetal bovine serum and penicillin/streptomycin for 24 hours and then switched to the same medium containing 500 μg/mL of G418. Media was exchanged every 48 hours. G418 resistant clones were transferred to 24-well tissue culture plates, and culture supernatants were tested for PK by ELISA. Lines expressing the highest level of recombinant PK were expanded in 2-L roller bottles. After reaching confluence, cells were washed with phosphate-buffered saline, and then a medium consisting of 80% Dulbecco Modified Eagle Media (High Glucose, with L-Glut and sodium pyruvate) 20% Cellgro complete serum free media (Mediatech), 10 μg/mL soybean trypsin inhibitor and 10 μg/mL limabean trypsin inhibitor was added to each roller bottle. Conditioned media were collected every 48-72 hours, supplemented with benzamidine to 5 mmol/L and stored at −20°C.

Four liters of conditioned media was filtered, supplemented with 50 mM sodium acetate, 1 mM EDTA and the pH was adjusted to 5.2 with acetic acid. Media was loaded onto a 100 mL S-Sepharose fast-flow cation exchange column equilibrated with 50 mmol/L sodium acetate, 1 mM EDTA, pH 5.2. The column was washed with 4 mM sodium acetate, 150 mM NaCl, pH 5.2 and eluted with a 1-L linear NaCl gradient (150 to 1,000 mM) in the same buffer. Samples of each fraction were run on a 10% polyacrylamide-sodium dodecyl sulfate (SDS) gel under non-reducing conditions followed by staining with Coomassie brilliant blue. PK containing fractions were pooled concentrated to a final volume of 1 mL using an Amicon Ultra 50K centrifugation filters (Amicon, Beverly, MA), dialyzed against TBS pH 7.4 and then stored at −80°C.

Assay of Proteolytic Activity

General proteolytic activity was measured using Ala-Pro-paranitroanilide (APpNA), as described previously [15]. To measure hydrolysis of APpNA, 5-10 μL (3 to 4 μg) of rPRCP1 was incubated in HEPES-carbonated buffer (137 mM NaCl, 3 mM KCl, 12 mM $NaHCO_3$, 14.7 mM HEPES, 5.5 mM glucose, 0.1% gelatin, 2 mM $CaCl_2$, 1 mM $MgCl_2$, 7.1 pH, filtered) buffer containing 1.0 mM APpNA, pH 7.1 at 37°C for 1 h in dark, unless otherwise stated.

Affinity of Chromogenic Substrates of rPRCP1

rPRCP1 was incubated in the presence of all synthesized chromogenic substrates (in duplicate) in HEPES-carbonated buffer containing a final concentration of 1 mM XP-paranitroanilide (pNA), where X denotes the selected amino acid and the other letters represents specific amino acid, and incubated at 37°C for 1 h. The liberation of

paranitroaniline from each substrate was determined by spectrophotometry at 405 nm. Assays were performed a minimum of 3 times.

Endothelial Cell Culture

Human pulmonary artery endothelial cells (HPAECs) were obtained and cultured in growth medium according to the recommendations of the supplier (Invitrogen, NY). Cells were subcultured onto Corning Costar culture 96 well plates (Pittsburgh, PA) and incubated overnight at 37°C.

Peptide Inhibition Studies of PK Activation on HPAEC

HEPES-carbonated buffer was used for washing steps and all dilutions. Cells were treated sequentially as follows with a 1 hour incubation periods and washing between steps: a) block with 1% gelatin to prevent non-specific binding of HK to the cell surface and the wells, b) 30 nM HK, c) 30 nM PK prepared with all concentrations of the peptide fragments tested, and d) addition of S2302 (0.8 mM final concentration) initiates measurement. All assays were run in triplicate a minimum of 3 times.

Colorimetric Assay for PRCP Inhibition

The initial rate of substrate hydrolysis was measured to determine rPRCPs or endothelial PRCP activity. Assays were carried out according to a previously published method with some modifications [9]. Changes in absorbance were measured with an ELX800 absorbance microplate reader from Bio-TEK (Winooski, VT). Assays were performed in triplicate.

Calculation of PRCP inhibition was quantified by the following equation:

$$\% \quad \text{Inhibition} = [1 - (\text{Sample} \quad \text{A}_\text{f} - Ab) / (\text{Total} \quad \text{A}_\text{f} - Ab)] \times 100$$

where A_f is the measured absorbance at 405 nm in the presence of any given peptide (potential inhibitor) and A_b is the absorbance of the blank solution.

IC_{50} values were also determined for inhibition of rPRCP activity through various peptides. Inhibitors were dissolved in HEPES-carbonated buffer (pH 6.0) or acetate buffer (pH 4.8) and were used to determine the type of inhibition and calculate the IC_{50} values. For the rPRCP, the incubation mixture at 37°C contained sub-saturating concentrations of substrate (relative to K_m of the given substrate).

Statistical Analysis

The parameters evaluated during this study were analyzed by Tukey's test or Newman-Keuls post-hoc (Prism Graph Pad 5.0, Graph Pad Software, Inc., USA).

RESULTS

Identification of an Optimal PRCP Chromogenic Substrate

Several chromogenic substrates were designed and synthesized based upon the sequence H-Gly-Proparanitroaniline (GPpNA) to select an optimal substrate to monitor PRCP activity.

The criteria used to design the substrate sequences were two-fold. First, the substrates must be distinct from one another. Second, the synthetic substrate ought to differ from that observed in protected dipeptides or GPpNA. The amino acid residues in the N-terminus of the substrate were selectively changed from an aliphatic to an aliphatic hydroxyl side chain, an aromatic, a basic side chain, or an acidic side chain (Fig. **1A**). The peptides prepared as PRCP substrates exhibited a similar primary structure, conforming to the sequence: xPpNA or yxPpNA (where x and y represent any amino acid, respectively, P is proline and pNA is paranitroaniline). The potency of each substrate sequence was quantified by measuring the ratio of its K_m to the K_m of GPpNA. A ratio smaller than 1 was considered more selective than GPpNA, while a ratio greater than 1 was considered less selective.

Initial studies showed that tripeptide substrates (EQPpNA or EWPpNA) were poorly cleaved by rPRCP1 based on the ratio of their K_m to the K_m of GPpNA (2.3-6.3); dipeptide substrates were preferred (Fig. **1A**). Studies next examined the contribution of aromatic (Trp) (ratio YPpNA/GPpNA=0.7), basic (His, Arg, or Lys) (0.6-2.2), acidic (Glu) (1.3-1.8), or polar uncharged (Asn, Gln) (2.5) residues at position X in xPpNA. The ratio of APpNA/GPpNA and TPpNA/GPpNA were similar and lower (0.4) (Fig. **1A**, **B**). The SPpNA/GPpNA ratio was found to be the lowest at 0.23 (Fig. **1A**, **B**). Further studies examined whether the addition of Gln (polar uncharged) to the N-terminus of SPpNA making a yxPpNA peptide improves substrate affinity. rPRCP-cleaved QSPpNA has a lower affinity than SPpNA (Fig. **1A**). These studies suggested that the decrease in the K_m for the hydrolysis of APpNA and SPpNA may be attributed to a better fit of the amino acid residue(s) in the active site of PRCP. Covalent docking of SPpNA and QSPpNA to the crystal structure of PRCP (PDB ID: 3N2Z) [17] revealed top-ranked results which bound at the S1 and S2 sub-sites in a manner consistent with our previously reported induced fit docking experiments [15] (Supplemental Fig. **1** (SF1)).

Plots of initial velocities versus substrate concentrations were fitted to the Michaelis-Menten equation to determine the K_m, k_{cat}, and k_{cat}/K_m values (Fig. **2A**, **B**). A representative plot of the release of pNA from SPpNA, APpNA, or GPpNA as function of the substrate concentration for rPRCP1 is shown (Fig. **2A**). As expected, the amount of pNA formed increased with the substrate concentration, obeying Michaelis-Menten kinetics. The product turnover (k_{cat}) of SPpNA was not significantly different than those of APpNA and GPpNA (Fig. **2B**). However since the K_M of SPpNA hydrolysis by rPRCP was 1.5 to 3.6 lower than that of APpNA and GPpNA, the catalytic efficiency (k_{cat}/K_m) of rPRCP hydrolysis of the chromogenic substrate SPpNA was at least 2-3-fold higher than APpNA and 6-7 times higher than GPpNA under our assay conditions, respectively (Fig. **2B**).

Since the C-terminus of human PK has the sequence $S^{636}PA^{638}$ and it has been proposed that it is a potential substrate for PRCP1 [14], we hypothesized that peptides of that sequence would interfere with rPRCP1 hydrolysis of APpNA. The pNA in SPpNA was changed to one of three amino acids (Ala, Pro, and Phe). Peptide SPA blocked the hydrolysis of APpNA by rPRCP1 in a concentration-dependent manner (Fig. **2C**). Angiotensin II and angiotensin III are the two substrates of PRCP1 [3, 16]. Since the C-termini of these molecules are Pro-Phe, the effect of SPF on APpNA metabolism was also determined. Unexpectedly, SPF was found to slightly inhibit the hydrolysis of APpNA at

concentrations > 2 mM, (Fig. **2C**). The reason for this is not clear, but the oxygen atom in Ser is capable of accepting hydrogen bonds from free NH groups, although such an interaction was not observed in a SPpNA docking study (Supplemental Fig. **1**) [18]. Finally, SPP was ineffective in inhibiting rPRCP1 (Fig. **2B**). Together, these observations support the notion that rPRCP1 has preference for alanine in the N-terminus of dipeptide substrates and the C-terminus of PK may be a substrate for PRCP1. These studies initiated investigations to map the enzyme-substrate interaction sites between PRCP1 and PK.

Identification of Sites on PRCP that Interact with PK

Next investigations determined whether the N-terminal domain of PRCP1 serves as an interaction site with PK. To test this hypothesis, five sequential 20-mers [^{41}LPAVAKNYSVLYFQQKVDHF^{60} (LPA20, Acc. No: NP_005031.1); ^{61}GFNTVKTFNQRYLVADKY WK^{80} (GFN20); ^{81}KNGGSILFYTGNEGDIIWFC^{100} (KNG 20); ^{101}NNTGFMWDVAEELKAMLVFA^{120} (NNT20); and ^{121}EHRYYGESLP FGDNSFKDSR^{140} (EHR20)] that span the entire N-terminal region of PRCP1 were synthesized by Quality Controlled Biochemicals, (Fig. **3A**). We determined which of these peptides blocked PK activation as detected by S2302 hydrolysis, but not PRCP1 hydrolysis of APpNA (Fig. **3A**).

Peptide LPA20 blocked PK activation when bound to HK by rPRCP with an IC_{50} value of 0.9 ± 0.3 mM (Fig. **3A**). This inhibition was concentration-dependent (Fig. **3B**). Additional studies determined that LPA20 did not block the hydrolysis of S2302 by plasma kallikrein indicating that the inhibition observed was not due to a direct effect on plasma kallikrein. Peptide EHR20 also blocked rPRCP activation of PK with an IC_{50} value of 3.2 ± 1.1 mM (Fig. **3A**). Dose-dependent effect of peptide EHR20 on PRCP1-dependent PK activation on endothelial cells is shown in (Fig. **3B**). Both peptides LPA20 and EHR20 cover an alpha helix that is a part of the dimerization region on PRCP1 (Supplemental Fig. **2**). PRCP1-induced PK activation was not significantly influenced by peptides GFN20, KNG20, and NNT20 (Fig. **3A**). None of the peptides corresponding to the N-terminus of PRCP1 had any effect on rPRCP1 activity, suggesting that LPA20 and EHR20 selectively interfere with PRCP1/PK binding sites (Fig. **3A**). These data suggested that a potential PK-binding site was localized to the amino-terminal region of PRCP1 and PRCP1 dimerization which may also be important in PK activation.

Additional studies found other sites on PRCP that influence PK activation. The active site pocket of PRCP1 is outlined by amino acid residues with neutral or hydrophobic side chain properties that participate in substrate recognition by PRCP. We investigated the inhibition of PRCP hydrolysis of two peptides SGQ16 and YPY14 that are adjacent to the opening of the active site pocket (Supplemental Fig. **2**) [17]. Peptide SGQ16 that contains the sequence SEXXXXS and spans the opening of the active site pocket blocked rPRCP activation of PK, but not rPRCP's hydrolysis of APpNA (Fig. **3A**, **C**, Supplemental Fig. **2**). SGQ16 inhibited PRCP1-dependent PK activation on cells with an IC_{50} value of 1.59 mM (Fig. **3A**). Peptide YPY14 that contains the sequence ...ASNFLQPL...that hangs over the active site pocket neither inhibited PK activation on cells nor APpNA hydrolysis (Fig. **3A**, **C**, and

Supplemental Fig. **2**). Our findings suggested that larger PK was more restricted in interacting with the active site pocket than smaller dipeptide substrates of PRCP.

Identification of Sites on PK that Interact with PRCP

In previous studies we observed that activation of PK by rPRCP1 resulted in an ~51 kDa heavy and two ~39 and 36 kDa light chains as detected on immunoblot, which was similar to the size of cleaved and reduced plasma kallikrein produced by FXIIa [9]. We proposed that PRCP1 might have endoproteinase activity. In order to test the hypothesis that the PRCP cleavage sites on PK are similar to that of FXIIa, we initially examined for the potential PRCP cleavage sites near R^{390}/I^{391}. Synthetic overlapping 8- to 10-mer peptides (PK residues 384-411) were screened for their abilities to block PRCP-dependent PK activation. Peptides that march through the RI activation site on PK (Accession No: P03952, EC 3.4.21.34), ^{384}TTKTSTRI^{391}, ^{387}TSTRIVGGT^{395}, ^{385}TKTSTRIVGGTN^{396}, ^{393}GGTNSSWGEWPW^{404}, ^{398}SWGEWPWQVSLQ^{409}, and ^{402}WPWQVSLQVK^{411}, did not block PK activation on cells or on microtiter plate cuvette wells in the presence of HK or inhibited rPRCP hydrolysis of APpNA (Fig. **4A**). Additional studies showed, however, that 100 μM peptide SWG12 which is adjacent to the RI cleavage site had the ability to inhibit ~15% of FXIIa (2 nM) hydrolysis of S2302 ($p < 0.05$) (Fig. **4B**). However, peptide TKT12 that spans the FXIIa RI cleavage site did not inhibit the enzyme. These data suggested that the mechanism of activation of PK by PRCP1 is distinct from FXIIa.

Studies on substrate recognition and the tripeptide SPA suggested that the extreme C-terminus of PRCP1 may be involved in the PRCP-PK interaction (Fig. **3**) [14]. Factor XI and PK are structurally very similar, but PRCP1 is incapable of activating factor XI. Since the last 10 amino acid residues [^{629}DGKAQMQSPA^{638} (DGK10)] at the C-terminal region of PK is missing in the C-terminus of factor XI, we focused on this region in PK activation by PRCP. Overlapping peptides corresponding to amino acids between Q^{607} and A^{638} of the proposed PRCP1 cleavage site on PK were synthesized to determine if any of these peptides blocked PRCP1-dependent PK activation on endothelial cells. Peptide DGK10 blocked PRCP1-dependent PK activation on endothelial cells with an IC_{50} of 3 mM (Fig. **4C**). DGK10 also blocked rPRCP with an IC_{50} value of 0.6 mM (Fig. **4D**). When the proline in DGK10 was substituted by alanine in ^{629}DGKAQMQS**A**A^{638} (DGK10M) inhibitory function was lost (Fig. **4C**, **D**). These data suggested that P^{637} and A^{638} on PK may also participate in its activation by rPRCP.

Investigations with rPK C-Terminal Mutants

In order to confirm that the C-terminus of PK is a substrate for PRCP, recombinant PK mutants were prepared with various mutations in the C-terminal SPA sequence. PK has a unique structure consisting of a heavy chain of 4 apple domains and a catalytic S1 peptidase domain (Fig. **5A**). Changes in the structure of PK were only made in the extreme C-terminal wild type SPA sequence by site-directed mutagenesis to SAA, SPX, or SAX where “X” represents a stop codon truncating the protein at the C-terminal amino acid (Fig. **5B**). Initial studies characterized these rPKs for their catalytic properties in comparison with purified plasma kallikrein and PK [19]. Human plasma kallikrein (2 nM) exhibited robust release of

pNA from S2302, while purified plasma human PK had none (Fig. **5C**). Alternatively, we observed that soluble recombinant wild-type PK, P637A, A638stop, and P637A/A638stop mutants after 1 h incubation in a microtiter plate cuvette which had significantly ($p \leq 0.0001$) higher kallikrein activity than that of wild-type PK (Fig. **5C**). Wild type rPK was easily activated by FXIIa (Fig. **5C**, Inset).

Since the rPKs developed some plasma kallikrein activity after 1 h incubation, we examined their ability to autoactivate. When assayed immediately, 25 nM purified plasma PK, wild type rPK, or any of the rPK mutants had no amidolytic activity indicating that there was no residual plasma kallikrein in the starting preparation of recombinant protein (data not shown). The addition of 25 nM rPK to the human plasma PK (25 nM) resulted in the same low level of plasma kallikein activity after 1 h incubation as wild type plasma PK alone (Fig. **5D**). Alternatively, incubation of wild type plasma PK (25 nM) with each of the mutant rPK C-terminal mutants (25 nM each) resulted in a significant amount ($p < 0.05$) of increased plasma kallikrein hydrolysis of S2302 (Fig. **5D**). The specificity of plasma kallikrein formation was shown by the ability of 100 nM of the plasma kallikrein inhibitor PF048 (PF04886847, kindly provided by Pfizer) to block these autoactivations of PK. Taken together, these results indicated that the P637A and P637A/A638stop mutants have a lower threshold for autoactivation of plasma PK than wild-type rPK.

Further investigations determined whether the soluble rPKs' activation is influenced by HK, a PK cofactor for activation on endothelium and artificial surfaces. In the presence of 25 nM HK, none of the 25nM rPKs preparation autoactivated in solution after 1 h incubation at 37°C (data not shown). These observations indicated that HK functioned to stabilize plasma PK from autoactivation in solution.

We examined the activation of wild-type PK alone versus the rPK mutants by rPRCP in microtiter plates when bound to HK coating the microtiter plate [10]. rPRCP (3 μg) activated 25 nM PK to plasma kallikrein is all cases after 1 h incubation (Fig. **6A**). Although equal concentrations of PK were added, the degree of activation of wild type rPK was about 66% to that of wild type plasma PK. rPK^{P637A} was significantly more activable by rPRCP than wild type rPK (Fig. **6A**). Additionally, both $rPK^{A638stop}$ and $rPK^{P637A/A638stop}$ were significantly less activable than rPK^{P637A} ($p<0.01$ and $p<0.05$, respectively (Fig. **6A**). The specificity of all these interactions were shown by the ability of 100 μM peptide SDD31 (the PK binding site on domain 6 of HK) to block rPRCP activation of PK and rPKs [20].

Moreover, studies determined the ability of each of the rPK mutants to activate plasma kallikrein when incubated with HK on human pulmonary artery endothelial cells (HPAEC) [21, 22]. Incubation of HK, purified plasma PK (PK), wild-type rPK, or the rPK mutants P637A, A638stop, or double mutant P637A/A638 alone with HPAEC did not result in S2302 hydrolysis (Fig. **6B**). When 25 nM HK was added along with each PK (25 nM) on HPAEC (25 nM), the wild-type plasma PK, wild type rPK, and the rPK mutants P637A, A638stop, or P637A/A638stop mutants were activated to plasma kallikrein (Fig. **6B**). Wild-type rPK (25 nM) activation to plasma kallikrein on HPAEC was less than half of that observed with an equal amount of purified plasma PK ($p<0.001$) (Fig. **6B**). Alternatively, the activation of each of the rPK mutants (25 nM) to plasma kallikrein was to a similar

extent as the activation of wild type plasma PK in the following order of efficacy: P637A> A638stop > P637A/A638stop > wild-type PK (Fig. **6B**). Activation of the $rPK^{P637A/A638stop}$ was significantly ($p \leq 0.05$) lower than the other mutants (Fig. **6B**). These data were similar to that observed with microtiter plate bound to HK (Fig. **6A**). The specificity of these activation experiments on HPAEC was shown by 90% inhibition with 150 μM PRCP inhibitor UM8190 (kindly provided by Dr. John Rimoldi). The combined rPK mutant activation studies on microtiter plates and HPAEC indicated that the C-terminal mutants of PK have more activable forms of PK and, regardless of mutation of the C-terminal PROVAL bond, rPRCP or endothelial cell PRCP is able to activate this rPK to plasma kallikrein. These data indicated that the C-terminal SPA sequence of PK is not the essential site for PRCP activation of PK.

FXIIa cleaves PK to produce alpha-kallikrein (α-kallikrein); plasma kallikrein cleaves PK to produce beta-kallikrein (β-kallikrein) [23]. Studies determined if the removal of C-terminal residue (Ala^{638}) of PK influenced its susceptibility to activation by FXIIa, plasma kallikrein or rPRCP. We initially carried out dose response and time course for each of the activator (FXIIa, plasma kallikrein or rPRCP) to obtain optimum activator concentration. These values were used in subsequent determinations of the extent and rates of activation of rPK mutants by each activator.

With each activating enzyme, the rate of rPK activation of the mutants was compared to wild- type rPK (Fig. **6C**). FXIIa (2 nM) activated wild-type PK (25 nM), P637A, A638stop, and P637A/A638stop to varying extents, thereby reaching a maximum level at 18-20 min (Fig. **6C**). While all mutant PKs were more sensitive to FXIIa-induced activation than the wild- type recombinant PK at an identical concentration of FXIIa, A638stop PK form had significantly ($p \leq 0.05$, n=4) enhanced sensitivity to FXIIa (Fig. **6C**).

Studies next sought to assess the sensitivity of recombinant mutant PKs to kallikrein-induced activation. Although normalized to equal enzyme and substrate concentrations, activation of the rPKs to plasma kallikrein by plasma kallikrein was lower than that observed with FXIIa (Fig. **6C**). Under the conditions of the assay, all mutant PKs were more sensitive to plasma kallikrein-induced activation than wild-type rPK reaching a maximum level within 8 h (Fig. **6C**). β-kallikrein has a significantly lower S2302 hydrolysis rate than α-kallikrein [23].

Last, investigations determined the activation of rPK mutants by rPRCP. Recombinant PRCP-induced rPK mutant activation reached maximum level within 8-11 h. The ability of rPRCP to activate wild type rPK or any of the mutants was the same.

DISCUSSION

These studies indicate that the interaction of PRCP1 with PK leading to PK activation is complex. PRCP1 interacts with PK in at least 3 locations, a region in its dimerization zone (peptide LPA20), an area orienting access to the active site pocket (peptide SGQ16), and its active site. While LPA20 and SGQ16 appeared to selectively inhibit the binding of PRCP1 to PK, GFN20, KNG20, or NNT20 was ineffective to inhibit the PRCP1-PK interaction at

the same molar concentration. Contrary to our hypothesis, a high concentration of LPA20 or SGQ16 peptide was required to block PRCP1-PK interaction. This observation cannot be readily explained. There are several possible explanations for the low affinity of LPA20 and SGQ16 for PK. Although short peptides are often lacking a stable conformation, average 10-20 amino acids in length are considered ideal for both structure/function studies and antibody preparation [24]. The presence of truncated peptide(s) in a product mixture containing long peptide could reduce the affinity of LPA20 or SGQ16 for PK. However, the HPLC chromatograms of LPA20 or SGQ16 product mixture indicate highly purified products. The formation of a cyclic peptide between the carboxyl and the N-terminal amine groups of LPA20 or SGQ16 also could provide another explanation for their lack of high affinities for PK, these peptides were identified on the basis of their retention times and molecular masses. Incorporation of D-amino acids or unusual amino acids into peptides may not only enhance binding affinity but tend to favor a cyclic conformation [25, 26]. However, there were no unnatural amino acids in LPA20 or SGQ16. The most likely explanation is that both LPA20 and SGQ16 may have multiple conformations in physiological buffer of which any of them is capable of interacting with PK [27].

On PK, PRCP1's actions are influenced by C-terminal peptide (DGK10) and peptide SPA, but rPK with mutagenized C-terminal proline-alanine is still a substrate of PRCP1. These data indicate that the C-terminus of PK contributes to its activation by PRCP1, but the C-terminus is neither necessary nor sufficient for PRCP1's PK activating activity. It is unexpected that peptides that march through the arginine-isoleucine bond that separates the apple domains of PK from its catalytic region have no influence on PRCP1 activation unlike that of FXIIa. This information strongly suggests that PRCP1 does not activate PK like FXIIa. This assessment is also supported by other studies.

In previous investigations, it was shown that PRCP1 activated PK bound to HK on plastic or endothelial cells with a K_m ~ 9 nM [10, 28]. In those experiments it appears that PRCP1 activates PK in a stoichiometric manner, i.e., it was a near equal molar concentration of PRCP that cleaved PK [10, 28]. Alternatively, factor XIIa activates PK with a K_m ~24 μM in a catalytic fashion with molar ratios of factor XIIa: PK of 1:100 to 200 [29]. Peptides (e.g. SWG12) that marched through the arginine-isoleucine region of PK inhibit factor XIIa but not PRCP1's activation of PK. In a previous work, Hooley *et al*. proposed that PRCP proteolysis of the C-terminus of PK allows for a molecular rearrangement of PK such that its active site becomes available as has been recognized for staphylocoagulase activation of plasminogen [14, 30]. Although peptides of the C-terminus of PK interfere with its activation by PRCP, the fact that rPKs with mutagenized C-terminus are still substrates of PRCP suggests that the C-terminal region is a modifier, but not essential, for PK activation. Other critical areas on PK must be involved in activation by PRCP.

The active site pocket of PRCP made up of Ser^{179}, Asp^{430} and His^{455} must be tightly regulated. In the development of optimal chromogenic substrates for PRCP, we found that smaller, less-charged amino acids serine, alanine, threonine, and histidine, in that order, were the leading N-terminal amino acids for XPpNA to provide the lowest K_ms (0.31 to 0.74 mM) (Fig. **1A**). SPpNA fits best into the active site pocket. Amino acids with bulky side chains were excluded. The finding that peptide SGQ16 that spans the active site pocket of

PRCP and blocks PRCP activation of PK supports the notion that a precise, tight fit into the active site region is essential for substrate specificity for PRCP.

The physiological role of PRCP in PK activation is not known. In $PRCP^{gt/gt}$ mice, PK is slightly but not significantly elevated, FXIIa is significantly decreased, but plasma BK levels are not different from normal [31]. This finding is distinctly different than that seen in $F12^{-/-}$ and $Kgn1^{-/-}$ (Kininogen KO mice) mice where plasma BK levels are reduced. Under conditions of angiotensin 2 receptor (AT2R) over-expression, there is increased PRCP mRNA and protein resulting in increased bradykinin formation that is blocked by AT2R receptor antagonists or plasma kallikrein inhibitors [12, 13]. These data suggest that PRCP activation of PK may be important for local, but not systemic bradykinin formation, but the precise physiological role needs further explanation.

Similarly, more is needed to be known concerning what are the physiological roles of plasma PK. PK has been known to be a cofactor for factor XII activation on surfaces and a major amplifying protease in the so-called contact activation system which is a defense mechanism for inflammatory events [32]. In the absence of PK, contact activation precedes albeit at a slower rate that corrects over time [33]. Hyperglycemic prekallikrein deleted mice ($Klkb1^{-/-}$) have reduced intracerebral hemorrhage in a direct injury model [34]. $Klkb1^{-/-}$ mice are also protected from ferric chloride-induced carotid artery thrombosis [35]. Likewise, prolonged PK inhibition by antisense oligonucleotides reduced thrombus formation, but acute pharmacological inhibition of PK results in an immediate prothrombotic state [31, 36, 37]. This information suggests that in chronic PK deficiency, there are some compensatory mechanisms that arise to give the animal a thrombosis protection phenotype. These data also suggest that PK has a real role in modifying thrombosis risk *in vivo* without a role in hemostasis since its deficiency is not associated with bleeding [33]. BK formation by PRCP activation of PK and BK's ability to elevate NO, prostacyclin, and tissue plasminogen activator (tPA) production contributes to thrombosis protection. However, chronic PK deficiency itself as seen in the $Klkb1^{-/-}$ mice and antisense oligonucleotide treatment is associated with thrombosis protection, suggesting that PK's influence thrombosis risk may be independent of bradykinin formation.

Unlike PK, much has been learned about the physiological functions of PRCP. $PRCP^{gt/gt}$ mice are constitutively hypertensive, thrombotic, and lean [2, 31, 37]. They have reduced angiogenesis, ischemia/reper-fusion repair, and hyper-inflammation upon vascular injury [37]. $PRCP^{gt/gt}$ mice also have improved glucose tolerance and less insulin resistance [38]. PRCP regulates energy metabolism in mice by reducing energy expenditure, reducing thyroid hormone, and brown adipose tissue uncoupling protein. Although there are several peptides known to be substrates for PRCP, the roles of two, $\alpha{-}MSH_{1\text{-}13}$ and angiotensin II, have precisely defined physiological activities. PRCP inactivates $\alpha MSH_{1\text{-}13}$ regulating murine anorexic activity [2]. In $PRCP^{gt/gt}$ mice, $\alpha{-}MSH_{1\text{-}13}$ accumulates in the hypothalamus and the animals are lean due to a heighten anorexic response [2]. PRCP also has been shown to be an equally important degrading enzyme of angiotensin II to make angiotensin-(1-7) in the kidney as angiotensin converting enzyme 2 [39]. However, in the presence of improved metabolism and leanness, $PRCP^{gt/gt}$ mice have an unhealthy cardiovascular system. It is not known completely how these seemingly disparate findings

will resolve. Angiotensin-(1-7) is involved in both adipogenesis and thrombosis protection [40-42]. Reduced PRCP contributes to leanness at two levels by increasing central anorexia and decreasing peripheral adipogenesis, and reducing anti-thrombosis protection from angiotensin-(1-7). It appears that before the modern era, PRCP may protect an animal from cardiovascular disease from heavy carbohydrate and fat ingestion needed to survive in periods of starvation.

In summary, the physical interaction between PRCP1 and PK for PK activation occurs at several regions in each protein. Since it is not essential for constitutive BK delivery, this enzyme-substrate interaction may have a precise role in vascular biology and metabolism. Characterization of the molecular basis of this interaction may lead to novel approaches for management of cardiovascular diseases and metabolic diseases.

Supplementary Material

Refer to Web version on PubMed Central for supplementary material.

ACKNOWLEDGEMENTS

The authors thank Dr. Jaya Mallela and Ms. Felicia Rabey for their technical assistance.

Sources of Funding

This work was supported by American Heart Association [0330193N] and National Institute of Health [SBAHQ-10-1-0309], and NASA/MSSGC to ZSM, and HL052779-17 and HL112666-02 to AHS.

ABBREVIATIONS

PRCP1	Prolylcarboxypeptidase isoform 1
rPRCP1	Recombinant PRCP
FXIIa	Activated factor XII
HK	High molecular weight kininogen
PK	Plasma prekallikrein
rPK	Recombinant PK
BK	Bradykinin
AT2R	Angiotensin 2 receptor
SDD31	PK binding site on domain 6 of HK
α-MSH$_{1-13}$	Alpha melanocyte stimulating hormone
tPA	Tissue plasminogen activator
UM8190	A PRCP inhibitor
APpNA	Ala-Pro-paranitroanilide
S2302	H-D-Pro-Phe-Arg-paranitroanilide

pNA Paranitroanilide

REFERENCES

1. Mallela J, Perkins R, Yang J, Pedigo S, Rimoldi JM, Shariat-Madar Z. The functional importance of the N-terminal region of human prolylcarboxypeptidase. Biochem Biophys Res Commun. 2008; 374:635–640. [PubMed: 18656443]
2. Wallingford N, Perroud B, Gao Q, et al. Prolylcarboxypeptidase regulates food intake by inactivating alpha-MSH in rodents. J Clin Invest. 2009; 119:2291–2303. [PubMed: 19620781]
3. Odya CE, Marinkovic DV, Hammon KJ, Stewart TA, Erdos EG. Purification and properties of prolylcarboxypeptidase (angiotensinase C) from human kidney. J Biol Chem. 1978; 253:5927–5931. [PubMed: 28321]
4. Zhao Y, Qiu Q, Mahdi F, Shariat-Madar Z, Rojkjaer R, Schmaier AH. Assembly and activation of HK-PK complex on endothelial cells results in bradykinin liberation and NO formation. Am J Physiol Heart Circ Physiol. 2001; 280:H1821–H1829. [PubMed: 11247797]
5. Wiggins RC. Kinin release from high molecular weight kininogen by the action of Hageman factor in the absence of kallikrein. J Biol Chem. 1983; 258:8963–8970. [PubMed: 6553057]
6. Colman RW, Mattler L, Sherry S. Studies on the prekallikrein (kallikreinogen)--kallikrein enzyme system of human plasma. I. Isolation and purification of plasma kallikreins. J Clin Invest. 1969; 48:11–22. [PubMed: 4974623]
7. Scott CF, Silver LD, Purdon AD, Colman RW. Cleavage of human high molecular weight kininogen by factor XIa in vitro. Effect on structure and function. J Biol Chem. 1985; 260:10856–10863. [PubMed: 3875612]
8. Lewis GP, Work T. Formation of bradykinin or bradykinin-like substances by the action of plasmin on plasma proteins. J Physiol. 1957; 135:7–8P. [PubMed: 13398981]
9. Moreira CR, Schmaier AH, Mahdi F, da MG, Nader HB, Shariat-Madar Z. Identification of prolylcarboxypeptidase as the cell matrix-associated prekallikrein activator. FEBS Lett. 2002; 523:167–170. [PubMed: 12123826]
10. Shariat-Madar Z, Mahdi F, Schmaier AH. Identification and characterization of prolylcarboxypeptidase as an endothelial cell prekallikrein activator. J Biol Chem. 2002; 277:17962–17969. [PubMed: 11830581]
11. Iwaki T, Castellino FJ. Plasma levels of bradykinin are suppressed in factor XII-deficient mice. Thromb Haemost. 2006; 95:1003–1010. [PubMed: 16732380]
12. Zhu L, Carretero OA, Liao TD, et al. Role of prolylcarboxypeptidase in angiotensin II type 2 receptor-mediated bradykinin release in mouse coronary artery endothelial cells. Hypertension. 2010; 56:384–390. [PubMed: 20606103]
13. Zhu L, Carretero OA, Xu J, et al. Angiotensin II type 2 receptor-stimulated activation of plasma prekallikrein and bradykinin release: role of SHP-1. Am J Physiol Heart Circ Physiol. 2012; 302:H2553–H2559. [PubMed: 22523247]
14. Hooley E, McEwan PA, Emsley J. Molecular modeling of the prekallikrein structure provides insights into high-molecular-weight kininogen binding and zymogen activation. J Thromb Haemost. 2007; 5:2461–2466. [PubMed: 17922805]
15. Chajkowski SM, Mallela J, Watson DE, et al. Highly selective hydrolysis of kinins by recombinant prolylcarboxypeptidase. Biochem Biophys Res Commun. 2011; 405:338–343. [PubMed: 21167814]
16. Mallela J, Perkins R, Yang J, Pedigo S, Rimoldi JM, Shariat-Madar Z. The functional importance of the N-terminal region of human prolylcarboxypeptidase. Biochem Biophys Res Commun. 2008; 374:635–640. [PubMed: 18656443]
17. Soisson SM, Patel SB, Abeywickrema PD, et al. Structural definition and substrate specificity of the S28 protease family: the crystal structure of human prolylcarboxypeptidase. BMC Struct Biol. 2010; 10:16. [PubMed: 20540760]

18. Richardson JS, Richardson DC. Amino acid preferences for specific locations at the ends of alpha helices. Science. 1988; 240:1648–1652. [PubMed: 3381086]
19. Friberger P, Gallimore MJ. Description and evaluation of a new chromogenic substrate assay kit for the determination of prekallikrein in human plasma. Adv Exp Med Biol. 1986; 198(Pt B):543–548. [PubMed: 3643742]
20. Chung DW, Fujikawa K, McMullen BA, Davie EW. Human plasma prekallikrein, a zymogen to a serine protease that contains four tandem repeats. Biochemistry. 1986; 25:2410–2417. [PubMed: 3521732]
21. Shariat-Madar Z, Rahimy E, Mahdi F, Schmaier AH. Overexpression of prolylcarboxypeptidase enhances plasma prekallikrein activation on Chinese hamster ovary cells. Am J Physiol Heart Circ Physiol. 2005; 289:H2697–H2703. [PubMed: 16113074]
22. Motta G, Rojkjaer R, Hasan AA, Cines DB, Schmaier AH. High molecular weight kininogen regulates prekallikrein assembly and activation on endothelial cells: a novel mechanism for contact activation. Blood. 1998; 91:516–528. [PubMed: 9427705]
23. Colman RW, Wachtfogel YT, Kucich U, et al. Effect of cleavage of the heavy chain of human plasma kallikrein on its functional properties. Blood. 1985; 65:311–318. [PubMed: 3871342]
24. Fuchs S, Kasher R, Balass M, et al. The binding site of acetylcholine receptor: from synthetic peptides to solution and crystal structure. Ann N Y Acad Sci. 2003; 998:93–100. [PubMed: 14592866]
25. Chen S, Gfeller D, Buth SA, Michielin O, Leiman PG, Heinis C. Improving binding affinity and stability of peptide ligands by substituting glycines with D-amino acids. Chembiochem. 2013; 14:1316–1322. [PubMed: 23828687]
26. Fletcher JT, Finlay JA, Callow ME, Callow JA, Ghadiri MR. A combinatorial approach to the discovery of biocidal six-residue cyclic D,L-alpha-peptides against the bacteria methicillin-resistant Staphylococcus aureus (MRSA) and E. coli and the biofouling algae Ulva linza and Navicula perminuta. Chemistry. 2007; 13:4008–4013. [PubMed: 17304598]
27. Bierzynski A. Methods of peptide conformation studies. Acta Biochim Pol. 2001; 48:1091–1099. [PubMed: 11995971]
28. Shariat-Madar Z, Mahdi F, Schmaier AH. Recombinant prolylcarboxypeptidase activates plasma prekallikrein. Blood. 2004; 103:4554–4561. [PubMed: 14996700]
29. Bernardo MM, Day DE, Olson ST, Shore JD. Surface-independent acceleration of factor XII activation by zinc ions. I. Kinetic characterization of the metal ion rate enhancement. J Biol Chem. 1993; 268:12468–12476. [PubMed: 8509386]
30. Friedrich R, Panizzi P, Fuentes-Prior P, et al. Staphylocoagulase is a prototype for the mechanism of cofactor-induced zymogen activation. Nature. 2003; 425:535–539. [PubMed: 14523451]
31. Adams GN, LaRusch GA, Stavrou E, et al. Murine prolylcarboxypeptidase depletion induces vascular dysfunction with hypertension and faster arterial thrombosis. Blood. 2011; 117:3929–3937. [PubMed: 21297000]
32. Colman RW, Schmaier AH. Contact system: a vascular biology modulator with anticoagulant, profibrinolytic, antiadhesive, and proinflammatory attributes. Blood. 1997; 90:3819–3843. [PubMed: 9354649]
33. Abildgaard CF, Harrison J. Fletcher factor deficiency: family study and detection. Blood. 1974; 43:641–644. [PubMed: 4821398]
34. Liu J, Gao BB, Clermont AC, et al. Hyperglycemia-induced cerebral hematoma expansion is mediated by plasma kallikrein. Nat Med. 2011; 17:206–210. [PubMed: 21258336]
35. Bird JE, Smith PL, Wang X, et al. Effects of plasma kallikrein deficiency on haemostasis and thrombosis in mice: murine ortholog of the Fletcher trait. Thromb Haemost. 2012; 107:1141–1150. [PubMed: 22398951]
36. Revenko AS, Gao D, Crosby JR, et al. Selective depletion of plasma prekallikrein or coagulation factor XII inhibits thrombosis in mice without increased risk of bleeding. Blood. 2011; 118:5302–5311. [PubMed: 21821705]
37. Adams GN, Stavrou EX, Fang C, et al. Prolylcarboxypeptidase promotes angiogenesis and vascular repair. Blood. 2013; 122:1522–1531. [PubMed: 23744584]

38. Jeong JK, Szabo G, Raso GM, Meli R, Diano S. Deletion of prolyl carboxypeptidase attenuates the metabolic effects of diet-induced obesity. Am J Physiol Endocrinol Metab. 2012; 302:E1502–E1510. [PubMed: 22454290]

39. Grobe N, Weir NM, Leiva O, et al. Identification of prolyl carboxypeptidase as an alternative enzyme for processing of renal angiotensin II using mass spectrometry. Am J Physiol Cell Physiol. 2013; 304:C945–C953. [PubMed: 23392115]

40. Than A, Leow MK, Chen P. Control of adipogenesis by the autocrine interplays between angiotensin 1-7/Mas receptor and angiotensin II/AT1 receptor signaling pathways. J Biol Chem. 2013; 288:15520–15531. [PubMed: 23592774]

41. Fraga-Silva RA, Pinheiro SV, Goncalves AC, Alenina N, Bader M, Santos RA. The antithrombotic effect of angiotensin-(1-7) involves mas-mediated NO release from platelets. Mol Med. 2008; 14:28–35. [PubMed: 18026570]

42. Fang C, Stavrou E, Schmaier AA, et al. Angiotensin 1-7 and Mas decrease thrombosis in Bdkrb2−/−mice by increasing NO and prostacyclin to reduce platelet spreading and glycoprotein VI activation. Blood. 2013; 121:3023–3032. [PubMed: 23386129]

A

Substrate sequence	rPRCP1 K_M(mM)	[$K_{M(Substrate)}/K_{M(GPpNA)}$]
Aliphatic		
H-Gly-Pro-pNA (GPpNA)	1.3±0.3	1
H-Ala-Pro-pNA (APpNA)	0.48±0.1	0.4
Aromatic		
H-Trp-Pro-pNA (WPpNA)	0.89±0.25	0.7
Hydrophilic		
Acidic		
H-Glu-Pro-pNA (EPpNA)	1.75±0.56	1.3
Basic		
H-Arg-Pro-pNA (RPpNA)	1.01±0.08*	0.8*
H-Lys-Pro-pNA (KPpNA)	2.86±0.13*	2.2*
H-His-Pro-pNA (HPpNA)	0.74±0.41	0.6
Neutral Polar		
H-Ser-Pro-pNA (SPpNA)	0.31±0.1	0.2
H-Thr-Pro-pNA (TPpNA)	0.48±0.08	0.4
H-Asn-Pro-pNA (NPpNA)	2.3±0.25	1.8
H-Gln-Pro-pNA (QPpNA)	3.2±0.65	2.5
Tripeptides		
H-Gln-Ser-Pro-pNA (QSPpNA)	2.3 ± 0.32	1.8
H-Glu-Gln-Pro-pNA (EQPpNA)	3.4± 0.48	2.6
H-Glu-Trp-Pro-pNA (EWPpNA)	6.29 ± 1.2	4.8

B

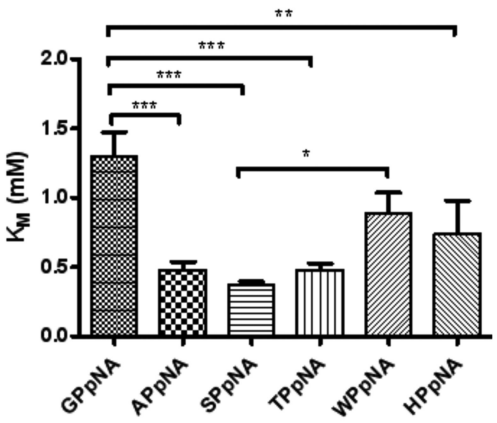

Fig. (1). Substrate specificity of rPRCP1

Panel A. K_M values of the hydrolysis of X-Pro-pNA by rPRCP1 and the ratio of hydrolysis against GPpNA are presented. Increasing concentrations of X-Pro-pNA substrates were incubated with rPRCP1 at 37°C for 1 hour. Two substrates marked by the asterisk required 24 hour incubation period. The hydrolysis of the substrates was detected at 405 nm. Panel **B**. Comparison of the K_M value of X-Pro-pNA. * denotes a significant ($P \leq 0.05$) difference in the mean compared to the mean of the counterpart. ** denotes a significant ($P \leq 0.01$) difference in the mean compared to the mean of the counterpart. *** denotes a significant ($P \leq 0.001$) difference in the mean compared to the mean of the counterpart.

A

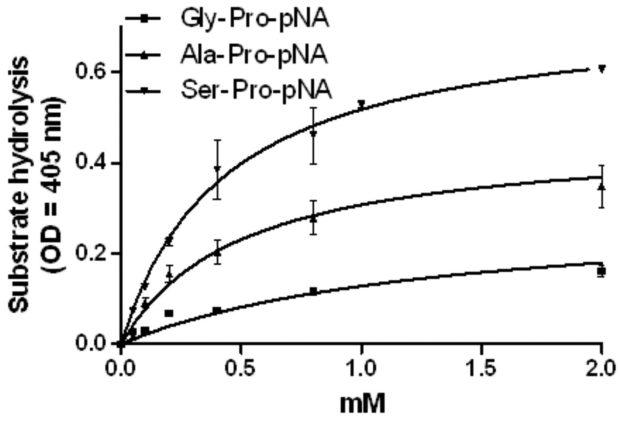

C

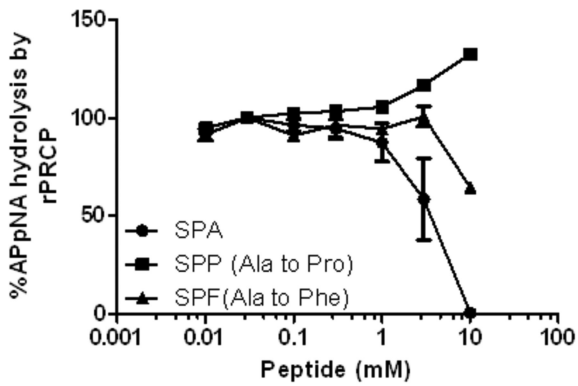

B

kinetics	Gly-Pro-pNA	Ala-Pro-pNA	Ser-Pro-pNA
K_m(mmol/L)	1.37 ± 0.2	0.580 ± 0.16	0.374 ± 0.040
V_{max} (μM/s)	0.0029 ± 0.007	0.0027 ± 0.002	0.0032 ± 0.0015
k_{Cat} (s^{-1})	0.0020 ± 0.004	0.0027 ± 0.003	0.0034 ± 0.002
k_{Cat}/K_m	0.0014 ± 0.002	0.0046 ± 0.001	0.0091 ± 0.002

Fig (2). Enzymatic characterization of recombinant PRCP by synthetic tripeptide derived from the C-terminus of PK

Panel **A**. Representative Michaelis–Menten curves for the determination of the K_m values for rPRCP1 on Gly-Pro-pNA, Ala-Pro pNA and Ser-Pro-pNA. Increased concentrations of each substrate were incubated with rPRCP1 at 37°C for 1 hour in dark. The releases of the para-nitroanaline were detected spectrophotometrically at 405 nm. Changes of absorbance were plotted versus substrate concentrations. Data were fit to the Michaelis-Menten equation using Prism Graphpad. Panel **B**. Kinetic parameters for the hydrolysis of X-Pro-pNA by rPRCP. Panel **C**. Substrate inhibition of rPRCP1. The amount of paranitroanalide formed by rPRCP from APpNA was determined by incubating each well with rPRCP1 in the absence or presence of increasing concentrations of SPA, SPP or SPF. The data are the mean ± S.E.M. of three experiments.

A

PRCP	Abbreviation	Sequence	S2302 hydrolysis IC_{50} (mM)	APpNA hydrolysis IC_{50} (mM)
N-terminus	LPA20	^{41}LPAVAKNYSVLYFQQKVDHF^{60}	0.91 ± 0.3	NE
	GFN20	^{61}GFNTVKTFNQRYLVADKYWK^{80}	NE	NE
	KNG20	^{81}KNGGSILFYTGNEGDIIWFC^{100}	NE	NE
	NNT20	^{101}NNTGFMWDVAEELKAMLVFA^{120}	NE	NE
	EHR20	^{121}EHRYYGESLPFGDNSFKDSR^{140}	3.2 ± 1.1	NE
Around active site	YPY14	^{291}YPYASNFLQPLPAW^{304}	NE	NE
	SGQ16	^{338}SGQVKCLNISETATSS^{353}	1.59 ± 0.5	NE

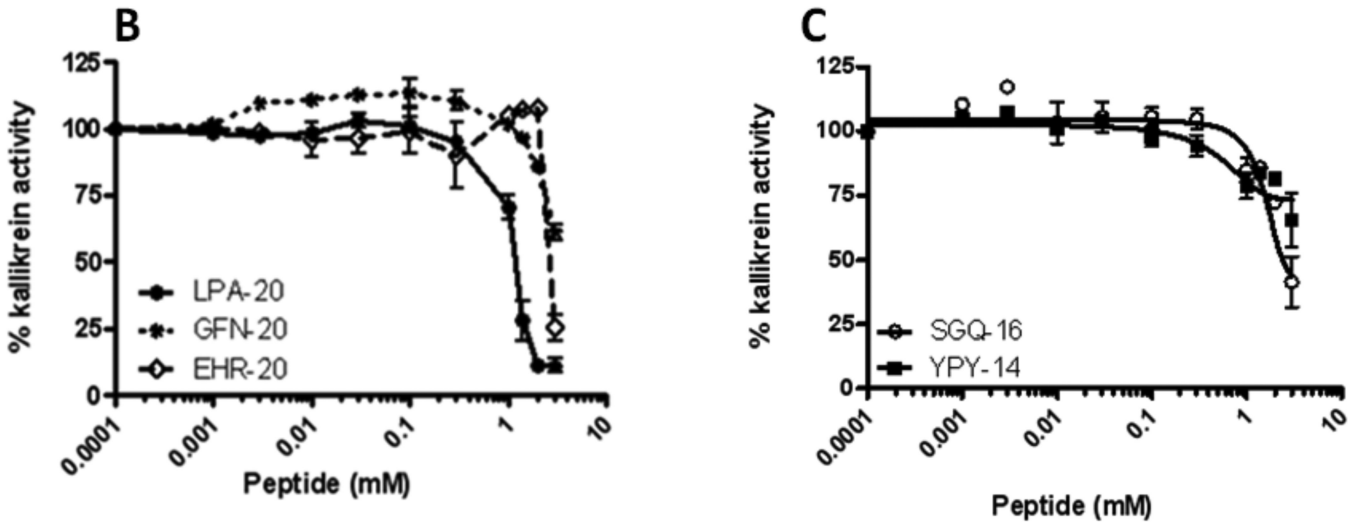

Fig. (3). Effects of synthetic oligopeptides corresponding to the N-terminus or active site of PRCP1 on PK activation in HPAEC

Panel **A** The inhibitory effects of peptides corresponding to the N-terminus or active site of PRCP1. IC_{50} was obtained for PRCP1 and PRCP1-depended kallikrein generation in the presence of the peptides. The hydrolysis of Ala-Pro-pNA (APpNA) by rPRCP1 in the presence of each peptide was compared to that of S2302 hydrolysis by PRCP1-depended PK activation. Panel **B**. Effects of LPA20, GFN20 and EHR20 peptides on PRCP1 - induced kallikrein generation on HPAEC. HPAEC (10^4 cells/well) were plated and cultured in 96 well plates. HPAEC were treated with HK (25 nM) for 1 h at 37°C. After washing, cells were incubated with PK (25 nM) in the absence or presence of increasing concentration of peptides (0.001–3.0 mM) for 1 h at 37°C. Cells then were washed three times to remove free PK and the peptides. Generated kallikrein was determined by cleavage of S2302. The level of S2302 hydrolysis was determined by measuring the absorbance of the reaction mixture in each well at OD 405 nm. The data are the mean ± S.E.M. of X experiments. Panel **C**. Effects of SGQ-16 and YPY-14 peptides on PRCP1-induced kallikrein generation on HPAEC.

Changes in pNA levels in cells were measured as described in Panel B. Data are presented as mean ± S.E.M. of X experiments.

A

Prekallikrein	Abbreviation	Sequence	S2302 hydrolysis IC_{50} (mM)	APpNA hydrolysis IC_{50} (mM)
FXIIa Cleavage site region				
	TTK8	^{384}TTKTSTRI^{391}	NE	NE
	TST9	^{387}TSTRIVGGT^{395}	NE	NE
	TKT12	^{385}TKTSTRIVGGTN^{396}	NE	NE
	GGT12	^{393}GGTNSSWGEWPW^{404}	NE	NE
	SWG12	^{398}SWGEWPWQVSLQ^{409}	NE	NE
	WPW10	^{402}WPWQVSLQVK^{411}	NE	NE
C-terminus				
	DGK10	^{629}DGKAQMQSPA^{638}	3	0.6
	DGK10M	^{629}DGKAQMQSAA^{638}	NE	NE

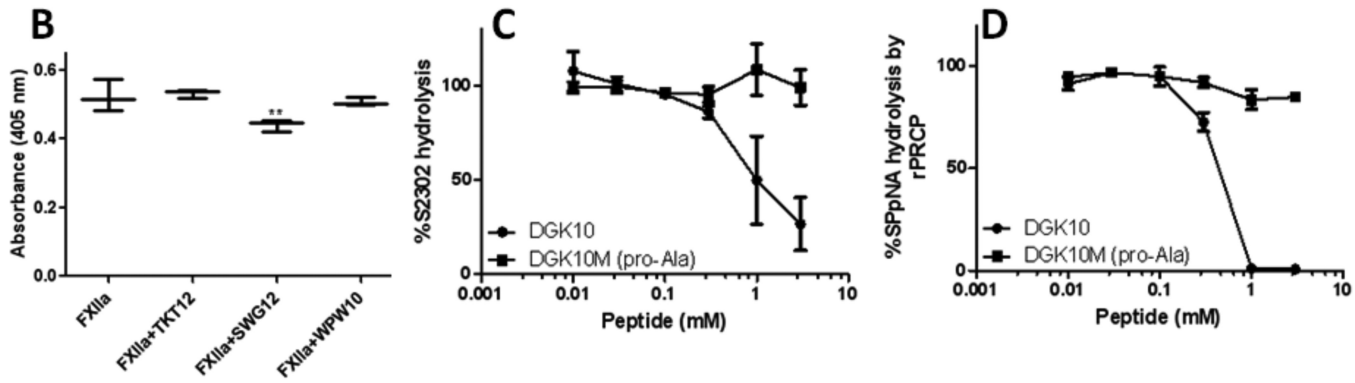

Fig. (4). Inhibition of PRCP1 by synthetic oligopeptides corresponding to the FXIIa cleavage site and C-terminus of human PK

Panel **A**. Characterization of of IC_{50} of synthetic oligopeptides and their effects on PRCP activity both on cells and in solution. Panel **B**. Effects of peptides corresponding to the FXIIa cleavage site on -FXIIa-induced PK activation as determined by S2302 hydrolysis. Panel **C**. Effects of peptides DGK10 and DGK10M on the formation of kallikrein on cells by PRCP1. Panel **D**. Effect of peptides DGK10 and DGK10M on the hydrolysis of APpNA by rPRCP1. NE; denotes no effect. * denotes a significant ($P \leq 0.05$) difference in the mean compared to control.

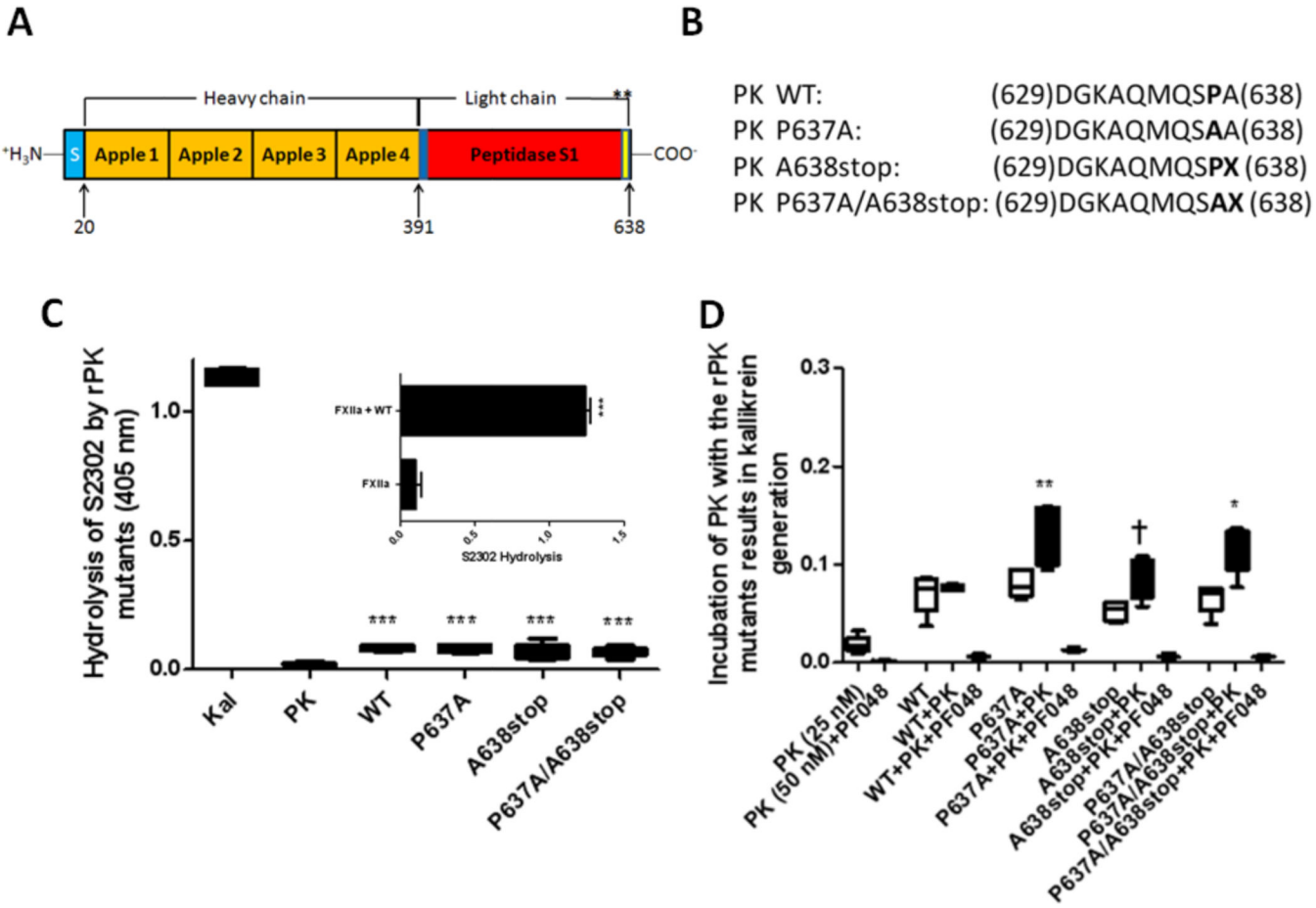

Fig (5). Activation and enzymatic characterization of recombinant PK mutants

Panel **A**. Map of the human plasma PK genomic RNA. The mutations that were introduced into PK (*KLKB1*) are indicated by asterisks. Arrows denote the beginnings or ends of PK chains. Mutations are represented by asterisks. The effects of the mutation of residues 637, 638, or a combination of the two in substrate hydrolysis were evaluated by comparing their activities to that of wild-type recombinant PK. Panel **B**. Diagram of the locations of the mutations that were introduced into PK. Sequence alignments are provided in PK wild-type. Wild-type PK and its C-terminal appropriate mutant sequence are shown. The number in parentheses flanking each amino acid sequence region indicates the position of the residue at the beginning and end of the region. Amino acids that were mutated in the wild-type PK to match the corresponding residue in the mutant rPK are indicated in bold. WT; wild-type, X; stop. Panel **C**. The wild-type PK and recombinant PK mutants do not release paranitroaniline (pNA) from S2302. Kallikrein (3 nM, positive control), PK (25 nM each), wild-type PK (25 nM), or rPK mutants (25 nM each) were incubated with S2302 (0.5 mM) in triplicate for 1 h at 37°C. Inset. The activation of wild-type rPK (25 nM) by XIIa (2 nM). The presence of pNA in each sample was measured by the change in absorbance at 405 nm using BioTek ELx800 Microplate Reader. Data are presented as mean ± S.E.M. of 3-5 experiments. ** $p < 0.0001$. Panel **D**. rPKs activate the human plasma PK in fluid-phase assay. PK (25 nM each), wild-type PK (25 nM), or rPK mutants (25 nM each) were incubated with PK (25 nM) in triplicate for 1 h at 37°C. After washing 3-times, the

generation of kallikrein in the absence or presence of PF-048 (PF-04886847, 0.3 μM, a kallikrein inhibitor) was assessed after 1 h at 37°C. Substrate hydrolysis was determined as described in Panel **C**. The amount of pNA was determined by measuring the change in absorbance at 405 nm using BioTek ELx800 Microplate Reader. * $P \leq 0.05$ compared to WT group. ** $P \leq 0.001$ compared to WT group. † $P \leq 0.05$ compared to P637A+rPRCP group.

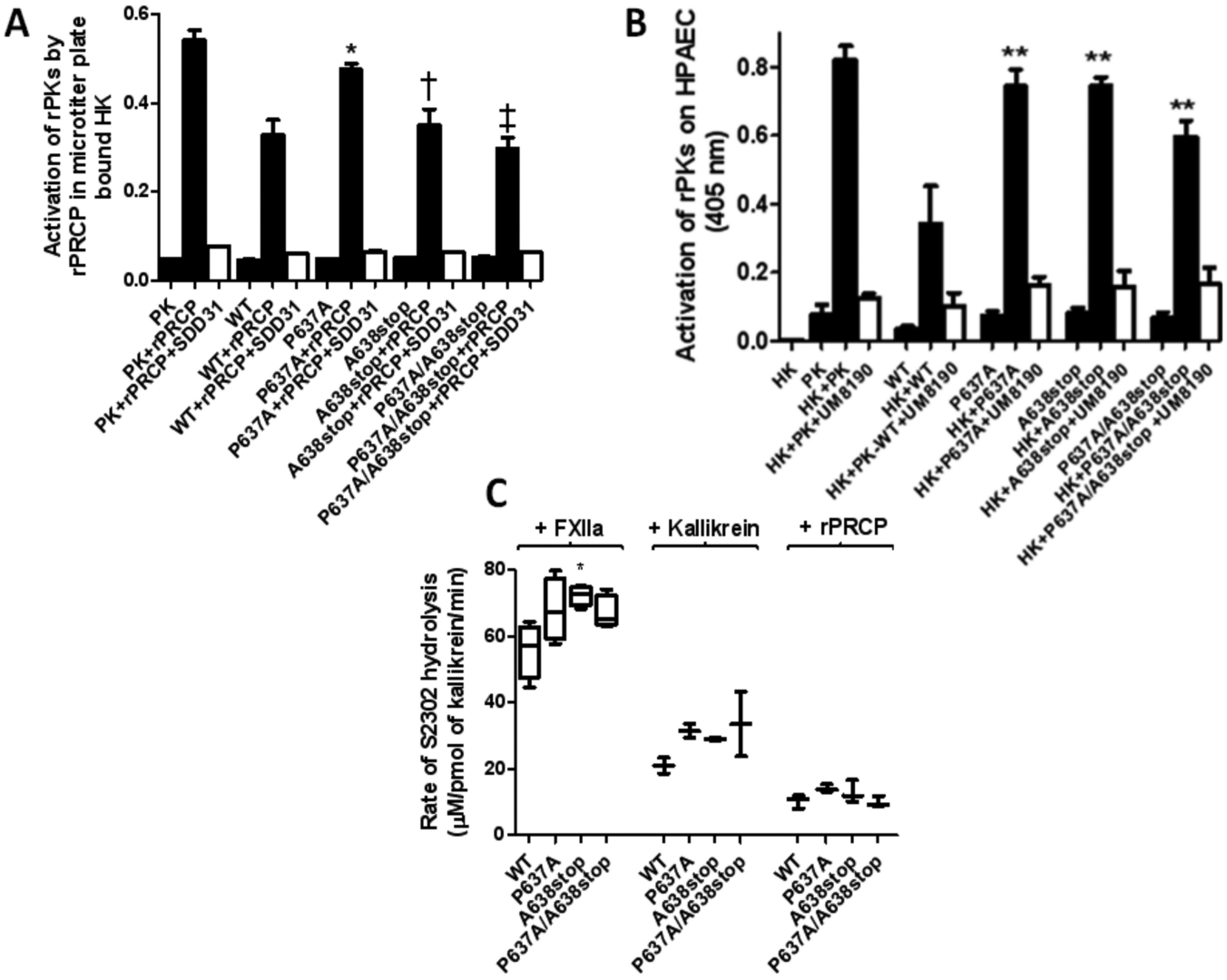

Fig. (6). Sensitivity of rPK mutants to activation

Panel **A**. Recombinant PRCP activates rPKs in microtiter plate bound to HK. HK-coated microtiter plate was treated with PK (25 nM); wild-type PK (25 nM), or rPK mutants (25 nM each) in the presence or absence of rPRCP (3 μg) and incubated at 37°C for 1 h in Hepes carbonate buffer, pH 7.1. The effect on activation of wild- type and the PK mutants in the absence or presence of SDD31(0.1 mM, blocks the binding of PK to HK) were determined by adding 0.5 mM of S2303 to each well and incubating at 37°C for 1 h. The generation of pNA from S2302 was read at wavelength of 405 nm. Data are presented as mean ± S.E.M. of three experiments. * $P \leq 0.05$ compared to WT + rPRCP group. † $P \leq 0.05$ compared to P637A + rPRCP group. ‡ $P \leq 0.01$ compared to P637A + rPRCP group. Panel **B**. Characterization of rPKs on HPAEC. HPAEC (3 x10^4 cells/well) were plated and cultured in 96 well plates. Triplicate samples of cells were incubated with HK (25 nM), PK (25 nM), rPKs (25 nM each), HK+PK (25 nM each), HK+wild-type PK (25 nM each), or HK+PK mutants (25 nM each). The generation of kallikrein in the absence or presence of UM8190 (0.1 mM, a PRCP inhibitor) was determined by measuring paranitroaniline (pNA) from S2302. Data are presented as mean ± S.E.M. of at least three experiments. ** denotes a

significant ($P \leq 0.01$) difference in the mean compared to P637A. Panel **C**. Activation of rPKs by FXIIa, kallikrein, or rPRCP. rPKs (25 nM each) was incubated in the presence of absence of FXIIa (2 nM), kallikrein (0.1 nM), or rPRCP (3 μg). The generation of α-kallikrein, β-kallikrein, or rPRCP-induced rPK mutants activation was determined by measuring a continuous production of pNA release from S2302 over time, and the slope of the time course was calculated by GraphPad Prism. The rate of S2302 hydrolysis was calculated by the following equation: rate of S2302= Slope/(S2302 extinction coefficient x pathlength). Data were mean ± SEM for 3-5 independent experiments normalized to control wells containing FXIIa, kallikrein, or rPRCP only. All data were statistically different from control ($P \leq 0.05$).